RELATIONSHIP BETWEEN TURBULENCE MODULATION AND SKEWNESS IN WALL BOUNDED FLOWS

Romain Mathis
Department of Mechanical Engineering
University of Melbourne, Victoria 3010, Australia
rmathis@unimelb.edu.au

Nicholas Hutchins & Ivan Marusic
Department of Mechanical Engineering
University of Melbourne, Victoria 3010, Australia
nhu@unimelb.edu.au, imarusic@unimelb.edu.au

ABSTRACT

Recent investigations into wall-bounded turbulent flows have shown a nonlinear scale interaction, whereby the large-scale motion amplitude modulates the small-scale structures (Hutchins & Marusic, 2007*b*). Mathis *et al.* (2009) developed a scheme to quantify the degree of modulation using a decoupling procedure, based on the Hilbert transformation applied to the filtered small-scale component of the fluctuating streamwise velocity; and highlighted the similarity between the wall-normal evolution of the degree of amplitude modulation and the skewness profile. This became the topic of study by Schlatter & Örlü (2010), who questioned this technique (at least at low Reynolds number) for unambiguously detecting and quantifying the effect of large-scale amplitude modulation of the small scales. The present study provides a complementary analysis of the relationship between the degree of amplitude modulation and the skewness using experimental and synthetic signals. It is shown that the Reynolds number trend in the skewness profile is related to the amplitude modulation of the small-scales by the large-scale signal.

Introduction

In wall-bounded turbulent flows, the near-wall region has attracted considerable attention based on the premise that it accounts for the highest levels of shear and turbulence production. However, most of these studies have been performed at low Reynolds numbers, tending to mask the effects of the outer-flow and large-scale motions. Over the past decade or so, the advent of innovative high-Reynolds number facilities (Hites, 1997; Zagarola & Smits, 1998; Osterlund, 1999; Nickels *et al.*, 2005), in conjunction with advances in numerical capability (Hoyas & Jiménez, 2006; Schlatter *et al.*, 2010), have provided fresh insights into inner/outer regions and scale interactions. There is accumulating evidence that large-scale events are universally present in wall-bounded flows (Hutchins & Marusic, 2007*a*; Monty *et al.*, 2007, 2009), and that they become increasingly more energetic as the Reynolds number increases. There is also evidence that as the Reynolds number increases the strength of the interaction between large-scales and the near-wall small-scales also increases. Particularly, it was suggested by Hutchins & Marusic (2007*b*), that in addition to the super-imposition effect of the large-scales onto the near-wall small-scales, these big motions seem to also have a distinct modulating influence. Complete discussions of these recent advances and other issues arising at high Reynolds numbers can be found in recent reviews by Marusic *et al.* (2010*b*) and Smits *et al.* (2011).

In our previous work (Mathis *et al.*, 2009), we proposed a decoupling procedure to quantify the amplitude modulation effect of the large-scale motion onto the small-scale structures. The single-point amplitude modulation coefficient, defined as the correlation coefficient between the filtered envelope of the small-scale fluctuations, $E_L(u_S^+)$, and the large-scale component, u_L^+, is of the form:

$$AM(z^+) = \frac{\overline{u_L^+ E_L(u_S^+)}}{\sqrt{\overline{u_L^{+2}}}\ \sqrt{\overline{E_L(u_S^+)^2}}} \qquad (1)$$

To obtain equation 1, the fluctuating streamwise velocity u^+ is first decomposed into a large- u_L^+ and a small-scale u_S^+ contribution, $u^+ = u_L^+ + u_S^+$, using a carefully chosen cut-off wavelength, $\lambda_x^+ = 7000$ (where λ is the streamwise wavelength, $\lambda_x^+ = \lambda U_\tau/\nu$, with U_τ the friction velocity and ν the kinematic viscosity). The filtered envelope of the small-scale contribution is obtained via a Hilbert transformation (see Mathis *et al.*, 2009, for full details). A typical trend of the wall-normal evolution of $AM(z^+)$, along with the skewness profile $Sk(z^+)$ of the streamwise velocity component, is given in figure 1 for Reynolds number $Re_\tau = 2800$ (where $Re_\tau = \delta U_\tau/\nu$, with δ the boundary layer thickness). In addition, as we noted in our previous work (Mathis *et al.*, 2009), $AM(z^+)$ exhibits remarkable (or surprising) similarities to the skewness profile $Sk(z^+)$.

Table 1. Experimental parameters for single-normal hot-wire experiments in the Melbourne wind tunnel.

Re_τ	x (m)	U_∞ (m/s)	δ (m)	U_τ (m/s)	ν/U_τ (μm)	l^+	l/d	ΔT^+	TU_∞/δ
2800	5	11.97	0.098	0.442	35.0	22	200	0.53	14 600
7300	21	10.30	0.319	0.352	44.0	23	200	0.34	17 400
19000	21	30.20	0.303	0.960	16.0	22	233	0.59	12 000

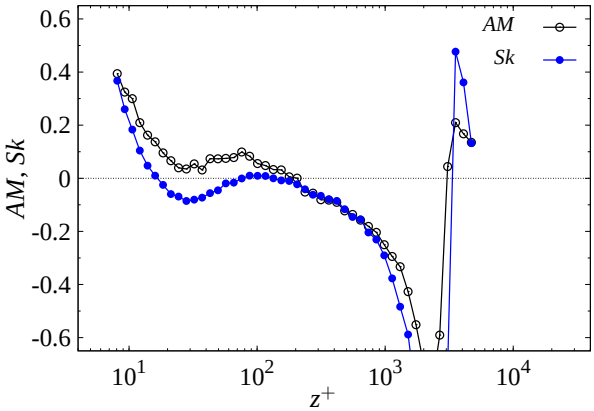

Figure 1. Wall normal evolution of the amplitude modulation coefficient *AM* and skewness factor *Sk*; $Re_\tau = 2800$.

Schlatter & Örlü (2010) attempted to investigate and explain this surprising similarity by means of experimental and synthetic signals. They show that the correlation coefficient *AM* used to quantify the amplitude modulation is related to the skewness *Sk* of the original signal. Due to such resemblance, they conclude that *AM* may not be an independent tool to unambiguously detect or quantify the effect of large-scale amplitude modulation of the small scales. However, it should be noted that their conclusions were restricted to relatively low Reynolds numbers, where there is limited scale-separation. Nevertheless their study raises valid questions about the strong similarity between both quantities, despite their clear fundamental differences (*Sk* is a measure of asymmetry in the probability distribution of a signal, and *AM* is the degree of amplitude modulation between small and large scales). To this end, here we will attempt to provide more information regarding this issue in order to remove potential ambiguities in the assessment of the amplitude modulation effect.

Experimental dataset

To investigate the relationship between the turbulence modulation and the skewness in wall-bounded flows, an experimental dataset obtained in the High Reynolds Number Boundary Layer Wind-Tunnel (also known as HRNBLWT) of the University of Melbourne is used. The setup and detailed results have been fully described in Hutchins *et al.* (2009) and Mathis *et al.* (2009). For consistency, we will briefly recall some of the boundary layer properties along with the main measurement characteristics. This facility consists of an open-return wind-tunnel with a working test section of $27 \times 2 \times 1$ m, and a free-stream turbulence intensity less than 0.05%. The pressure gradient is maintained to zero along the working test section by bleeding air from the tunnel ceiling through adjustable slots. Further details of the facility can be found in (Hafez *et al.*, 2004), and Nickels *et al.* (2005). Measurements of the streamwise fluctuating velocity were conducted by means of a single-normal hot-wire probe. The probe is made from platinum Wollaston wire of various diameters, operated in a constant temperature mode using an overheat ratio of 1.8. For each Reynolds number the diameter d and length l of the sensing element were adjusted in order to maintain a constant viscous scaled length of $l^+ = lU_\tau/\nu \simeq 22$, with $l/d = 200$ as recommended by Ligrani & Bradshaw (1987). Such arrangement allows comparison without any spatial resolution influences, a recurrent issue in wall-bounded flow measurements (see Hutchins *et al.*, 2009). To adequately resolve both the smallest- and largest-scales, a non-dimensional sample interval was set in the range $\Delta T^+ \simeq 0.3 - 0.6$, with a total length of the velocity sample T in the range $12000 - 18000$ boundary layer turnover times (defined in outer scaling TU_∞/δ where U_∞ is the freestream velocity). Table 1 gives the full details of the experimental conditions, where x refers to the distance between the tripped inlet and the measurements stations. The friction velocity U_τ was calculated from a Clauser chart fit (using log-law constants $\kappa = 0.41$ and $A = 5.0$) which has been confirmed with oil-film interferometry measurements (Chauhan *et al.*, 2010). Boundary layer thickness is calculated from a modified Coles law of the wake fit (Jones *et al.*, 2001).

Amplitude modulation versus skewness

Mathis *et al.* (2009) and Schlatter & Örlü (2010) both made use of synthetic signals to demonstrate the robustness of *AM* and to show its intimate link to *Sk*. These synthetic signals, both fundamentally different, are useful to understand further the relationship between the turbulence modulation and the skewness factor. Here we briefly present the main characteristics of these signals. The synthetic signal used by Mathis *et al.* (2009) for validation purposes, is constructed using the original signal in which the phases of the corresponding Fourier coefficients have been replaced (scrambled) with a randomly generated number between 0 and 2π. Hence, this operation preserves the energy spectra distribution of the signal as well as the variance. However, this operation removes all asymmetrical information, resulting in a zero skewness distribution. This synthetic signal, u_{sc}, is referred to hereafter as the *"scrambled signal"*. The synthetic signal introduced by Schlatter & Örlü (2010) is also constructed from a real measurement, only in which the whole signal has been shuffled. Hence, this operation conserves all probabilities of the signal (variance, skewness and flatness), but the structural

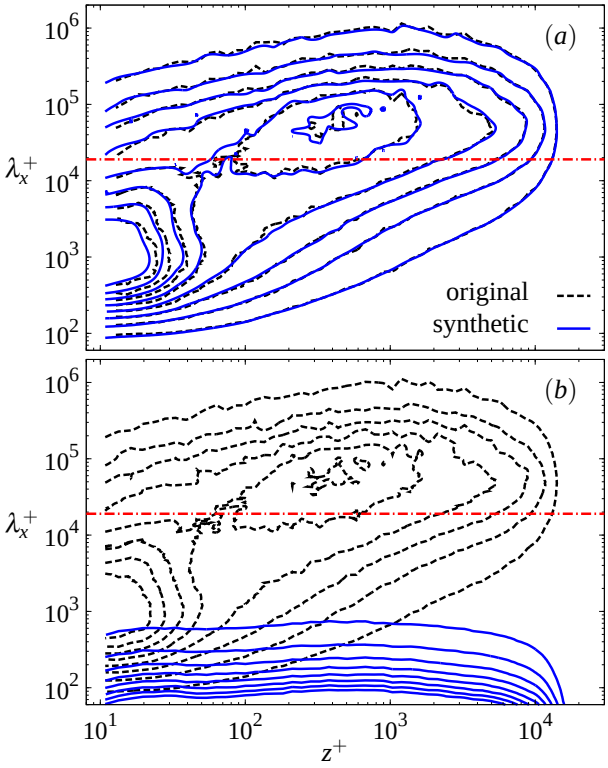

Figure 2. Iso-contours of pre-multiplied energy spectra of the streamwise velocity fluctuations $k_x\phi_{uu}/U_\tau^2$ ($Re_\tau = 19000$); Levels are from 0.2 to 1.8 in steps of 0.2; (a) measured signal compared to scrambled signal; (b) measured signal compared to shuffled signal; The horizontal red dot-dashed line shows the location of the spectral filter $\lambda_x^+ = 7000$.

information about spatial scales is lost. This synthetic signal, u_{sh}, is referred to hereafter as the *"shuffled signal"*. The energy content of both synthetic signals, compared to the original measurement used to constructed them, is shown in figure 2. It should be noted that the scrambled signal u_{sc} retains all characteristics of the energy content of a turbulent flow even if the skewness is set to zero (Fig. 2*a*). This means that the structural information and the range of scales are conserved. On the other hand, the shuffled signal u_{sh} has all its energy weighted towards the smaller-scales (as in white-noise) while retaining asymmetrical information (Fig. 2*b*). Therefore, the range of scales is reduced to just small-scale events, which is unrealistic for a turbulence signal, particularly in wall-bounded flows. One should also note that since the shuffled signal contains only small-scales, the notion of applying a scale decomposition becomes somewhat meaningless. (The cut-off wavelength used in the amplitude modulation characterisation scheme developed by Mathis *et al.* (2009) is noted by the horizontal red dot-dashed line in figure 2.)

Despite the unphysical nature of their shuffled signal, Schlatter & Örlü (2010) applied to it a scale decomposition and the amplitude modulation diagnostic tool. A comparison of the wall-normal evolution of the coefficient of modulation *AM* is given in figure 3 for the original and synthetic signals. For the discussion, the skewness profile of the original signal has also been added to the figure. It should be noted

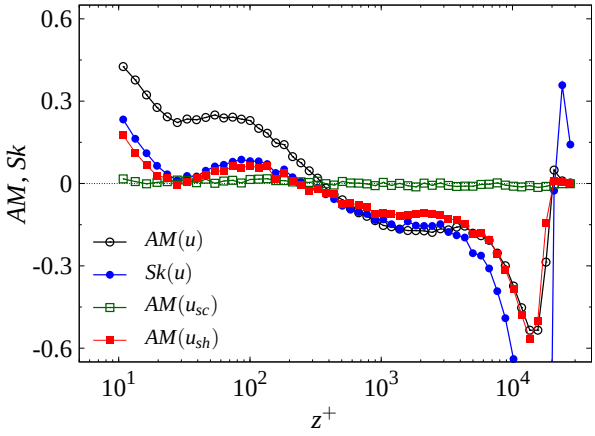

Figure 3. Wall-normal evolution of the amplitude modulation coefficient *AM* for the original and synthetic signals, and skewness profile *Sk* of the original signal; $Re_\tau = 19000$.

that these results correspond to high Reynolds number data from the University of Melbourne ($Re_\tau = 19000$), thus avoiding issues and possible misinterpretations due to limited scale-separation. As can be seen in figure 3, *AM* and *Sk* are clearly separated and cannot be confused when the Reynolds number becomes sufficiently high. However, as shown by Schlatter & Örlü (2010), the amplitude modulation coefficient applied to the shuffled signal does return a high degree of resemblance to the skewness profile, whereas in the case of the scrambled signal the modulation coefficient returns zero. It is noted that while the large-scale energy content of the shuffled signal is nearly zero (as well as the energy of the filtered envelope of the small-scale, involved in Eqn. 1), it still returns a significant degree of modulation. Such a result may be due to the fact that the diagnostic tool *AM* is simply a correlation coefficient between the large-scales and the filtering envelope of the small-scales, which can return, as occurs here, a significant degree of modulation even if their energy is low. In this respect, the formulation of the amplitude modulation coefficient given in equation 1 may not be, *technically* as robust as we originally claimed in Mathis *et al.* (2009), and likely a refined version of *AM* would need to be developed. Based on this, Schlatter & Örlü (2010) claimed that this method *"may not be an independent tool to unambiguously detect or quantify the effect of large-scale amplitude modulation of the small-scales"*. However, it should be kept in mind that the first step of the amplitude modulation diagnostic tool consists of a scale separation operation and as clearly stated in Mathis *et al.* (2009), the chosen cut-off wavelength should be carefully selected according to the pre-multiplied energy spectra map of the considered signal. But, as seen in figure 2(b), applying a scale-decomposition below and above $\lambda_x^+ = 7000$ makes no sense in the case of the shuffled signal. Therefore, in the case of turbulent flow, such ambiguity is unlikely to occur as long as each step of the modulation diagnostic tool is carefully applied. Nevertheless, Schlatter & Örlü (2010) have clearly shown that the *AM* coefficient and the skewness factor are somehow related, which is not surprising as the amplitude modulation would introduce or increase asymmetry in signals. Therefore, the amplitude modulation diagnostic may provide a framework to interpret the Reynolds number trend of the

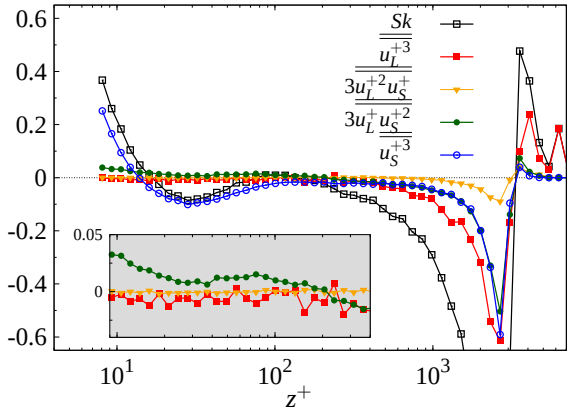

Figure 4. Wall-normal evolution of the expansion terms of the skewness factor; $Re_\tau = 2800$.

skewness factor profile, which will be discussed in the next section.

The decomposed skewness profile

To understand further the relationship between the correlation coefficient *AM* and the skewness factor *Sk*, it is useful to consider the expansion of *Sk* using the decomposed signal $u^+ = u_L^+ + u_S^+$,

$$Sk = \frac{\overline{u^{+3}}}{\left(\overline{u^{+2}}\right)^{3/2}} = \frac{\overline{u_L^{+3}} + 3\overline{u_L^{+2}u_S^+} + 3\overline{u_L^+u_S^{+2}} + \overline{u_S^{+3}}}{\left(\overline{u^{+2}}\right)^{3/2}}, \quad (2)$$

which can be written as

$$Sk = \overline{\overline{u_L^{+3}}} + 3\overline{\overline{u_L^{+2}u_S^+}} + 3\overline{\overline{u_L^+u_S^{+2}}} + \overline{\overline{u_S^{+3}}}, \quad (3)$$
$$\text{with } \overline{\overline{X}} = \overline{X} / \left(\overline{u^{+2}}\right)^{3/2},$$

and such decomposition has been considered before by Sreenivasan *et al.* (1999).

The wall-normal evolution of each term of the decomposed skewness factor is given in figure 4 for $Re_\tau = 2800$. The small-scales term $\overline{\overline{u_S^{+3}}}$ appears to account for the majority of the skewness factor up to $z^+ = 200$, whereas the other terms seem to have little contribution (we are not considering in the discussion the wake region, where intermitence effects are dominant). Furthermore, it is observed in the insert of figure 4 that the cross term $3\overline{\overline{u_L^+u_S^{+2}}}$ also has a non-negligible contribution, the two other terms appearing to be zero or nearby. To gain a better understanding of the role of each dominant terms of the decomposed skewness factor, the wall-normal evolution of *Sk*, $\overline{\overline{u_S^{+3}}}$ and $3\overline{\overline{u_L^+u_S^{+2}}}$ are plotted in figure 5 for several Reynolds numbers. The Reynolds number trend of *Sk* has been previously established over a large range of Reynolds number, from laboratory facilities to atmospheric surface layers (Metzger & Klewicki, 2001). Particularly, as the Reynolds number increases, a change in sign of the minima occurring in the buffer region has been observed, as shown in figure 5(a)

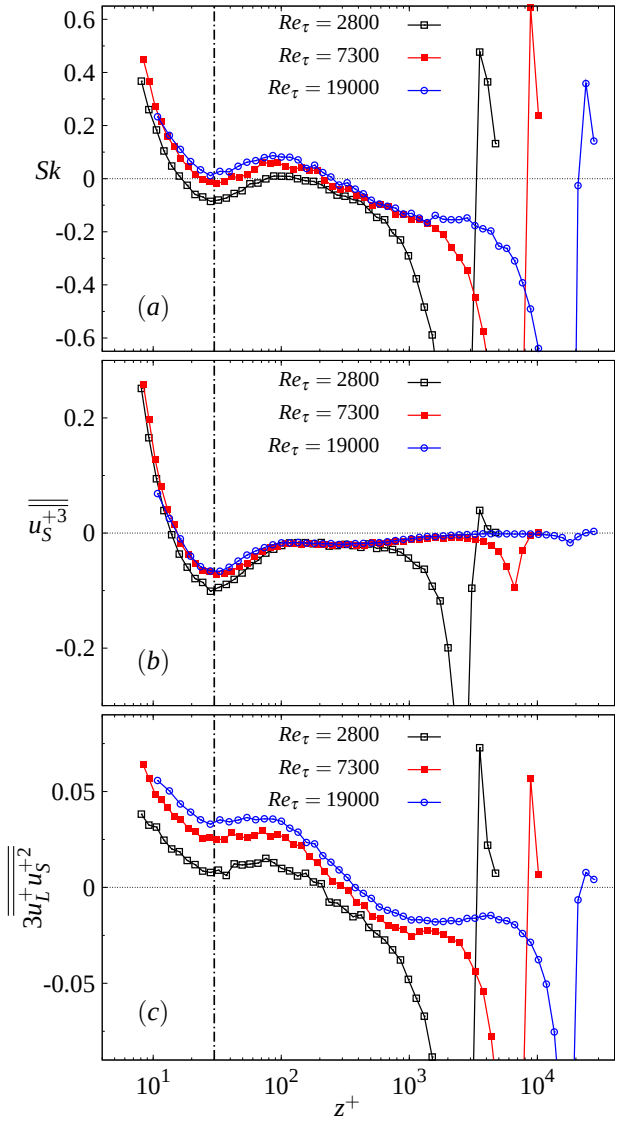

Figure 5. Reynolds number trend of (a) the skewness factor *Sk* and dominant terms of the expansion of the skewness factor, (b) $\overline{\overline{u_S^3}}$ and (c) $3\overline{u_L u_S^2}$; The vertical dot-dashed line marks the location of the minima of the *Sk* profile.

(the vertical dot-dashed line marks the location of the minima). The reasons for such behaviour remain unclear. The small-scale term $\overline{\overline{u_S^{+3}}}$ appears to contribute only to the rise of this minima (Fig. 5*b*). In contrast, $3\overline{\overline{u_L^+u_S^{+2}}}$ appears to be the most sensitive term to the increasing Reynolds number. A strong rise of the profile is observed all the way through the boundary layer, in the buffer layer particularly, with values nearly four times higher between $Re_\tau = 2800$ and $Re_\tau = 19000$. What is more remarkable is the high degree of resemblance of this profile to the profile of the amplitude modulation coefficient *AM*. This is even more evident by plotting them together as shown in figure 6. In other words, this suggests that the cross-term $3\overline{\overline{u_L^+u_S^{+2}}}$ of the skewness factor expansion might be used as an alternative or complementary diagnostic tool to *AM*, to quantify the level of amplitude mod-

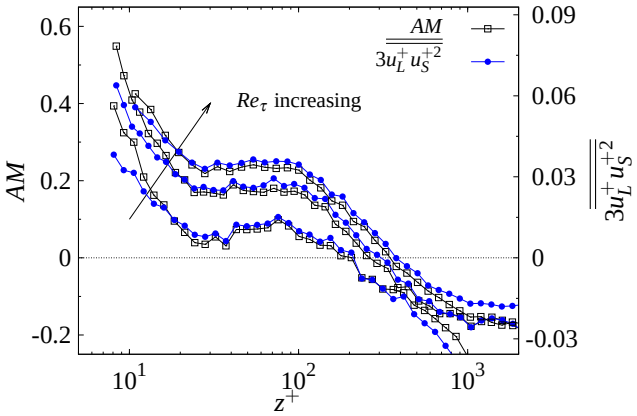

Figure 6. Wall-normal evolution of the amplitude modulation coefficient *AM* (left hand-side vertical axis) and the cross term $3\overline{\overline{u_L^+ u_S^{+2}}}$ of the skewness factor expansion (right hand-side vertical axis), for Reynolds numbers $Re_\tau = 2800$, 7300 and 19000.

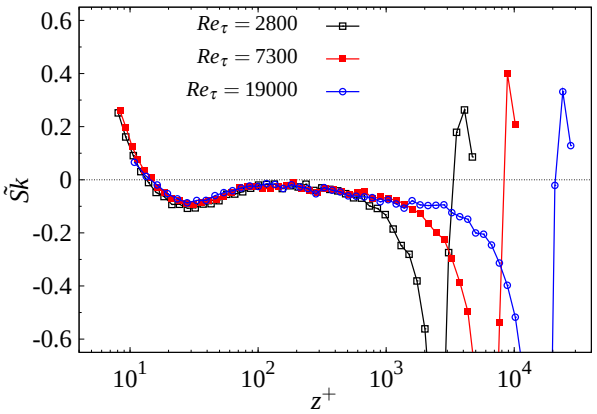

Figure 7. Reconstruction of the skewness factor without the cross term $3\overline{\overline{u_L^+ u_S^{+2}}}$, e.g. $\tilde{Sk} = \overline{\overline{u_L^{+3}}} + 3\overline{\overline{u_L^{+2} u_S^+}} + \overline{\overline{u_S^{+3}}}$.

ulation of the small-scales by the large-scales. This is not so surprising given that it is similar to a small-scale envelope (u_S^{+2}), correlated with a large-scale component (u_L^+). Having established this, it also suggests that the Reynolds number trend of the skewness factor is closely related to rising amplitude modulation effect as Re_τ increases. Indeed, it is now known that the large-scale motions strengthen with increasing Reynolds number, and so too does the amplitude modulation effect (Mathis *et al.*, 2009), which is shown here to contribute to the rise of the skewness factor. In fact, a reconstruction of the skewness factor without the cross-term $3\overline{\overline{u_L^+ u_S^{+2}}}$, e.g. $Sk = \overline{\overline{u_L^{+3}}} + 3\overline{\overline{u_L^{+2} u_S^+}} + \overline{\overline{u_S^{+3}}}$, shows an invariant skewness factor over one order of magnitude in Reynolds number, as seen in figure 7, as opposed to the trend observed in figure 5(*a*).

Amplitude modulation in turbulence modelling

Interesting observations about the relationship between *AM* and *Sk* can also be made using the predictive model recently proposed by Marusic *et al.* (2010*a*):

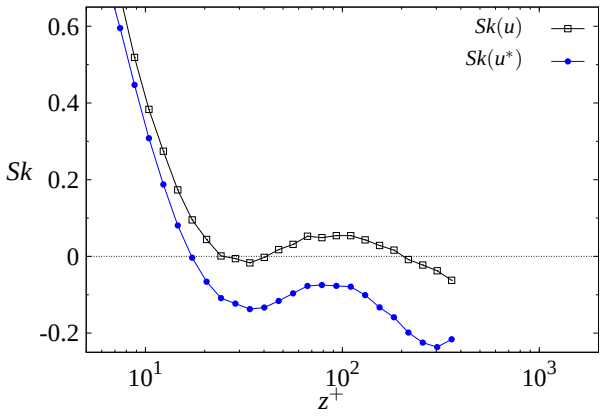

Figure 8. Wall-normal evolution of the skewness factor for the original and universal signals; $Re_\tau = 7300$.

$$u_p^+(z^+) = u^*(z^+)\left\{1 + \beta u_{OL}^+\left(z_O^+, \theta_L\right)\right\} + \alpha u_{OL}^+\left(z_O^+, \theta_L\right) \quad (4)$$

where u_p^+ is the predicted statistically-representative streamwise fluctuating velocity signal in the inner region, u^* the universal signal, and α, β and θ_L are calibrated parameters. The only input required in the equation is the fluctuating large-scale streamwise velocity signal u_{OL}^+ from a position in the log-region. The model consists of two parts, the first part modelling the amplitude modulation at z^+ by the large-scale log-region motions, and the second part modelling the superposition of these large-scale motions felt at z^+. The originality of this empirical model is that it is built based on a universal signal u^*, which is defined as the idealised signal that would exist in a turbulent boundary layer in the absence of any large-scales influence. Therefore, this signal has no amplitude modulation or superposition effects from large-scale events. This universal signal has been determined from a calibration measurement performed at high Reynolds number ($Re_\tau = 7300$), in which the original signal is de-trended (removing the superposition effect) and then de-modulated to obtain u^*. Full details about the model and its construction are available in Mathis *et al.* (2011).

An interesting property of u^* is that the signal, which has been de-trended and de-modulated, maintains a non-zero skewness factor, as shown in figure 8. However, u^* contains no sign of modulation, as it has been defined such that $AM(u^*) = 0$. (It should be noted that scrambling or shuffling this signal will also return a zero modulation coefficient.) This shows that the amplitude modulation defined by the diagnostic tool *AM* is not purely a consequence of any asymmetry information contained in a turbulent signal, as was suggested by Schlatter & Örlü (2010). Furthermore, as the amplitude modulation effect is removed in the universal signal, the skewness factor is lowered, which reinforces our previous conclusion that the Reynolds numbers trend of *Sk* is a consequence of large-scale turbulence modulation. Indeed, it has been shown in Mathis *et al.* (2011) that the universal signal is statistically representative of a low Reynolds number turbulent boundary layer ($Re_\tau \simeq 1000$), even if it has been built from a high Reynolds number case ($Re_\tau = 7300$).

Finally, it is worth noting that the modelling of the amplitude modulation in equation 4 is an essential element in the prediction of the skewness factor, and more generally in all

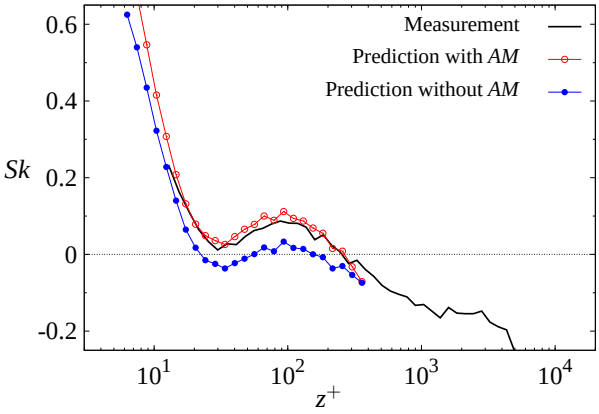

Figure 9. Prediction of the skewness factor with and without amplitude modulation modelled; $Re_\tau = 19000$.

odd moments. An example of prediction with and without the amplitude modulation effect is given in figure 9. Without the amplitude modulation component the skewness is improperly predicted. Typically, the Reynolds number trend of the skewness factor would not be captured and all predictive odd moments would remain invariant at any Reynolds numbers considered.

Conclusion

The relationship between the large-scale amplitude modulation and the skewness factor in wall-bounded flow has been extensively studied by means of synthetic signals and scale-decomposition. It is shown that the diagnostic tool *AM* developed by Mathis *et al.* (2009) to quantify the amplitude modulation of the small-scale structures by the large-scale motions works well if applied with care and to realistic turbulent signals. It is emphasised that the scale-decomposition, constituting the first step of the method, must be sensibly applied based on the energy content of the turbulent signal considered. A closer analysis of the relative contribution of the large- and small-scales to the skewness factor shows that the cross-term of the expansion, $3\overline{\overline{u_L^+ u_S^{+2}}}$, is closely related to the *AM* coefficient, and can be used as an alternative diagnostic tool. Furthermore, the amplitude modulation effect appears to be the only cause of the rise of the skewness factor as the Reynolds number increases.

REFERENCES

Chauhan, K. A., Ng, H. C. H. & Marusic, I. 2010 Empirical mode decomposition and Hilbert transforms for analysis of oil-film interferograms. *Meas. Sci. Tech.* **21** (105404), 1–13.

Hafez, S., Chong, M. S., Marusic, I. & Jones, M. B. 2004 Observations on high Reynolds number turbulent boundary layer measurements. In *Proc. 15th Australasian Fluid Mech. Conf*. AFMC00200.

Hites, M. H. 1997 Scaling of high-reynolds number turbulent boundary layers in the national diagnostic facility. PhD thesis, Ill. Inst. Technol.

Hoyas, S. & Jiménez, J. 2006 Scaling of the velocity fluctuations in turbulent channels up to $Re_\tau = 2003$. *Phys. Fluids* **18**, 011702.

Hutchins, N. & Marusic, I. 2007*a* Evidence of very long meandering features in the logarithmic region of turbulent boundary layers. *J. Fluid Mech.* **579**, 1–28.

Hutchins, N. & Marusic, I. 2007*b* Large-scale influences in near-wall turbulence. *Phil. Trans. R. Soc. Lond. A* **365**, 647–664.

Hutchins, N., Nickels, T., Marusic, I. & Chong, M. S. 2009 Spatial resolution issues in hot-wire anemometry. *J. Fluid Mech.* **635**, 103–136.

Jones, M. B., Marusic, I. & Perry, A. E. 2001 Evolution and structure of sink-flow turbulent boundary layers. *J. Fluid Mech.* **428**, 1–27.

Ligrani, P. M. & Bradshaw, P. 1987 Spatial resolution and measurement of turbulence in the viscous sublayer using subminiature hot-wire probes. *Exp. Fluids* **5**, 407–417.

Marusic, I., Mathis, R. & Hutchins, N. 2010*a* Predictive model for wall-bounded turbulent flow. *Science* **329** (5988), 193–196.

Marusic, I., McKeon, B. J., Monkewitz, P.A., Nagib, H. M., Smits, A. J. & Sreenivasan, K. R. 2010*b* Wall-bounded turbulent flows: Recent advances and key issues. *Phys. Fluids* **22**, 065103.

Mathis, R., Hutchins, N. & Marusic, I. 2009 Large-scale amplitude modulation of the small-scale structures in turbulent boundary layers. *J. Fluid Mech.* **628**, 311–337.

Mathis, R., Hutchins, N. & Marusic, I. 2011 A predictive inner-outer model for streamwise turbulence statistics in wall-bounded flows. *J. Fluid Mech.* **In Press**.

Metzger, M. M. & Klewicki, J. C. 2001 A comparative study of near-wall turbulence in high and low Reynolds number boundary layers. *Phys. Fluids* **13**, 692–701.

Monty, J. P., Hutchins, N., Ng, H. C. H., Marusic, I. & Chong, M. S. 2009 A comparison of turbulent pipe, channel and boundary layer flows. *J. Fluid Mech.* **632**, 431–442.

Monty, J. P., Stewart, J. A., Williams, R. C. & Chong, M. S. 2007 Large-scale features in turbulent pipe and channel flows. *J. Fluid Mech.* **589**, 147–156.

Nickels, T. B., Marusic, I., Hafez, S. & Chong, M. S. 2005 Evidence of the k_1^{-1} law in high-Reynolds number turbulent boundary layer. *Phys. Rev. Lett.* **95**, 074501.

Osterlund, J. M. 1999 Experimental studies of zero pressure-gradient turbulent boundary layer. PhD thesis, KTH, Stockholm.

Schlatter, P., Li, Q., Brethouwer, G. & Hennningson, A. V. Johanssonand D. S. 2010 Simulations of spatially evolving turbulent boundary layers up to $re_\theta = 4,300$. *Int. J. Heat Fluid Flow* **31** (3), 25161.

Schlatter, P. & Örlü, R. 2010 Quantifying the interaction between large and small scales in wall-bounded turbulent flows: A note of caution. *Phys. Fluids* **22** (5), 051704.

Smits, A. J., McKeon, B. J. & Marusic, I. 2011 Highreynolds number wall turbulence. *Annu. Rev. of Fluid Mech.* **43**, 353–375.

Sreenivasan, K. R., Dhruva, B. & San Gil, I. 1999 The effects of large scales on the inertial range in high-Reynolds-number turbulence. In *eprint arXiv:chao-dyn/9906041*, pp. 6041–+.

Zagarola, M. V. & Smits, A. J. 1998 Mean-flow scaling of turbulent pipe flow. *J. Fluid Mech.* **373**, 3379.